SCIENTIFIC REP⚙RTS

The Growth Mechanism of Transition Metal Dichalcogenides by using Sulfurization of Pre-deposited Transition Metals and the 2D Crystal Hetero-structure Establishment

Chong-Rong Wu[1,2], Xiang-Rui Chang[2], Chao-Hsin Wu[1] & Shih-Yen Lin[1,2]

A growth model is proposed for the large-area and uniform MoS_2 film grown by using sulfurization of pre-deposited Mo films on sapphire substrates. During the sulfurization procedure, the competition between the two mechanisms of the Mo oxide segregation to form small clusters and the sulfurization reaction to form planar MoS_2 film is determined by the amount of background sulfur. Small Mo oxide clusters are observed under the sulfur deficient condition, while large-area and complete MoS_2 films are obtained under the sulfur sufficient condition. Precise layer number controllability is also achieved by controlling the pre-deposited Mo film thicknesses. The drain currents in positive dependence on the layer numbers of the MoS_2 transistors with 1-, 3- and 5- layer MoS_2 have demonstrated small variation in material characteristics between each MoS_2 layer prepared by using this growth technique. By sequential transition metal deposition and sulfurization procedures, a $WS_2/MoS_2/WS_2$ double hetero-structure is demonstrated. Large-area growth, layer number controllability and the possibility of hetero-structure establishment by using sequential metal deposition and following sulfurization procedures have revealed the potential of this growth technique for practical applications.

With the advantage of theoretically predicated ultra-high carrier mobility values, graphene is believed to be of potential application for high-speed electronics in the below 10 nm technology node[1,2]. However, due to its zero-bandgap nature, graphene transistors usually exhibited low ON/OFF ratios. This disadvantage has substantially limited the practical application of graphene for logic circuits. To overcome this disadvantage of graphene, people have gradually turned their focus to other two-dimensional (2D) crystals with bandgaps such as transition metal dichalcogenides (TMDs) in recent years[3–5].

One of the promising TMDs for the transistor application is Molybdenum disulfide (MoS_2)[6,7]. Although its mobility value is much lower than graphene, MoS_2 transistors with high ON/OFF ratios around 10^8 have already been demonstrated, which has revealed the potential of MoS_2 for the transistor application[8–10]. One promising approach to obtain this material is the traditional mechanical exfoliation[11]. Although MoS_2 flakes with high crystalline quality can be obtained by using this method, uniform and large-area MoS_2 films are still required for the practical application. In nowadays, the mainstream method to grow large-area TMD films is the chemical vapor deposition (CVD). By using either MoO_3 or $MoCl_5$ as the precursor, MoS_2 films can be synthesized in hot furnace with the co-evaporation of sulfur (S) powder at 700–850 °C[12,13]. With graphene/sapphire samples as the substrates, MoS_2/graphene hetero-structures have also been demonstrated prepared by CVD for device applications[14].

[1]Graduate Institute of Electronics Engineering, National Taiwan University, No. 1, Sec. 4, Roosevelt Rd., Taipei 10617, Taiwan. [2]Research Center for Applied Sciences, Academia Sinica, No. 128, Sec. 2, Academia Rd., Taipei 11529, Taiwan. Correspondence and requests for materials should be addressed to S.-Y.L. (email: shihyen@gate.sinica.edu.tw)

Although CVD is very promising for large-area MoS$_2$ growth, there are still several limitations for this technique. Since the transition metal precursor and the S powder are uniformly distributed onto the substrates at high growth temperature, selective growth is difficult to achieve with the traditional CVD growth technique. In this case, when dealing with more complicated 2D crystal hetero-structures, selective etching to expose contact areas for electrodes would become a necessary processing procedure for device fabrications. Until now, there is no such report regarding selective etching of 2D crystals in literature. On the other hand, for the preparation of different TMDs to establish 2D crystal hetero-structures, different precursors have to be adopted. In this case, growth optimizations are required for each 2D crystal, which will further complicate the growth procedure of the 2D crystal hetero-structure. Therefore, if a standard growth procedure can be applied to different TMD growth, the establishment of 2D crystal hetero-structures would become much easier and more promising for practical applications[15]. In previous publications, it has been demonstrated that by sulfurizing pre-deposited Mo films in hot furnace, large-area MoS$_2$ films can be grown on sapphire substrates[16–19]. By using the similar approach, large-area WS$_2$ can also be prepared[19,20]. Therefore, we believe that by repeating the sequential transition metal deposition and the sulfurization procedures, large-area and uniform TMD hetero-structures may be prepared. To achieve this goal, further investigation over the growth mechanisms of sulfurizing pre-deposited transition metal films in hot furnace is required.

In this paper, we have investigated the growth mechanisms of large-area MoS$_2$ films by sulfurizing pre-deposited Mo thin films at 750 °C. By fixing the thickness of Mo films at 1 nm and decreasing the sulfur supply, similar Raman peak differences are observed. The results suggest that the same MoS$_2$ layer numbers are obtained for samples grown under different amounts of sulfur powder. The picture obtained by using cross-sectional high-resolution transmission electron microscopy (HRTEM) is adopted to investigate the actual layer numbers and film morphologies of the MoS$_2$ samples. With the observation of small Mo oxide clusters on the surface for the sample grown under the sulfur deficient condition, a growth model is proposed to explain the growth mechanisms of the MoS$_2$ films by using the sulfurization of pre-deposited Mo films. By sequential transition metal deposition and sulfurization procedures, we have also demonstrated a WS$_2$/MoS$_2$/WS$_2$ double hetero-structure grown through this growth method.

Results and Discussions

Characterizations of MoS$_2$ grown by using different amounts of sulfur powder.

The Raman spectra of the MoS$_2$ samples prepared by using sulfurization of 1.0 nm Mo with 2.5, 2.0 and 1.5 g sulfur powder are shown in Fig. 1(a). As shown in the figure, two characteristic Raman peaks are observed for the three samples with one peak E$_{2g}^1$ located at 384 cm^{-1} and the other A$_{1g}$ at 408 cm^{-1}. They are associated with the in-plane and out-of-plane vibration modes of the MoS$_2$ crystal, respectively[21]. It has also been reported that the frequency difference between the two peaks would increase from ~21 cm^{-1} to >24 cm^{-1} for single-layer to >4-layer MoS$_2$ films[13]. The Raman peak differences Δk of the three samples grown by using sulfur powder 2.5, 2 and 1.5 g are 24.14, 24.37 and 24.50 cm^{-1}, respectively. The results suggest that although different amounts of sulfur powder are adopted, similar MoS$_2$ layer numbers around 4–5 layers are obtained for the three samples. The phenomenon also indicates that the layer numbers of the MoS$_2$ films prepared through this approach is determined by the pre-deposited Mo film thicknesses. It has been proposed in previous publications that MoS$_2$ films with better crystalline quality would result in reduced E$_{2g}^1$ full width at the half maximum (FWHM) value and enhanced E$_{2g}^1$/A$_{1g}$ peak ratios[12,22]. The FWHM values of the E$_{2g}^1$ peak are 3.55, 3.4 and 2.48 cm^{-1}, while the E$_{2g}^1$/A$_{1g}$ peak intensity ratios are 0.57, 0.51 and 0.65 for the three samples, respectively. The smallest E$_{2g}^1$ FWHM value and the highest E$_{2g}^1$/A$_{1g}$ peak intensity ratio are observed for the sample prepared by using 1.5 g sulfur power. The results suggest that 1.5 g sulfur is the optimized growth parameter for the sulfurization of 1.0 nm Mo film. The picture of the sample sulfurized by using 1.5 g sulfur power is shown in Fig. 1(b). A blank sapphire substrate is also shown in the figure for comparison. The picture has revealed a uniform and large-area MoS$_2$ film grown on the sapphire substrate, which has demonstrated the potential of this technique for wafer-scale TMD growth. To confirm the layer number of the MoS$_2$ film, the cross-sectional HRTEM image of the sample grown by using 1.5 g sulfur powder is shown in Fig. 1(c). As shown in the figure, 5-layer MoS$_2$ is clearly observed for the sample. The results are consistent with the observation obtained from the Raman spectra.

The MoS$_2$ film grown under the sulfur deficient condition.

To further investigate the growth mechanism for the sulfurization of pre-deposited Mo films, an additional sample with no sulfur supply is prepared for comparison. Since there is always residue sulfur accumulation near the downstream of the growth chamber after repeating growth cycles, it is expected that a small amount of sulfur will still diffuse to the sample surface and result in MoS$_2$ growth. However, under such a sulfur deficient condition, not all the pre-deposited Mo will be transformed into MoS$_2$. The cross-sectional HRTEM image of the sample prepared with no sulfur supply is shown in Fig. 2(a). As shown in the figure, clusters of materials instead of flat 2D crystal films spreading over the sample surface are observed. To further investigate this phenomenon, the HRTEM image with a higher magnification of the same sample is shown in Fig. 2(b). It seems that the sample surface including the small clusters is still covered by few-layer MoS$_2$. To verify the chemical compositions of the small clusters, high-angle annular dark field (HAADF) mappings of elements Mo, sulfur (S), oxygen (O) and Aluminum (Al) are shown in Fig. 2(c). The mapping picture of Al would indicate the location of the sapphire substrate. As shown in the figure, besides a thin layer of the Mo and S signals observed above the sapphire substrate, the signals of the two elements are also observed on the cluster. The results may suggest that few-layer MoS$_2$ fully cover the sample surface including the clusters. The phenomenon is consistent with the observation of the cross-sectional HRTEM image shown in Fig. 2(b). On the other hand, beside the sapphire substrate, the O signal is also observed on the clusters. Since the cluster may be fully covered with few-layer MoS$_2$, it is possible that the S signal observed on the clusters comes from the covering few-layer MoS$_2$ films. In this case, it is reasonable to assume that the clusters contain mostly Mo
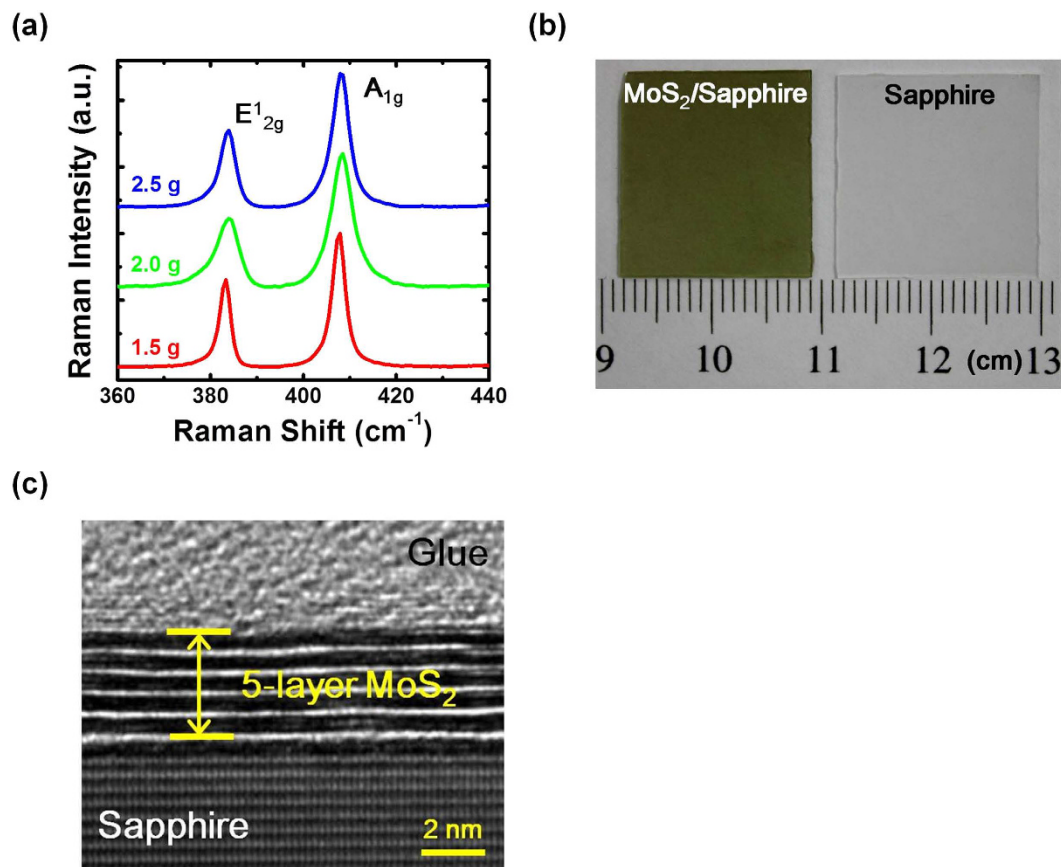
Figure 1. (**a**) The Raman spectrums of the MoS$_2$ samples prepared by using sulfurization of 1.0 nm Mo with 2.5, 2.0 and 1.5 g sulfur powder. (**b**) The picture and (**c**) the cross-sectional HRTEM image of the sample grown with 1.5 g sulfur powder. A blank sapphire substrate is also shown in (**b**) for comparison.

oxides. The other phenomenon observed in Fig. 2(b) is that there seems to be MoS$_2$ films underneath the small Mo oxide clusters. To verify this phenomenon, the cross-sectional HRTEM images of the sample with 0°, 5°, 10° and 15° tilt angles from the cross-sectional view are shown in Fig. 2(d). It is clearly seen from the figures that the Mo oxide clusters are covered with few-layer MoS$_2$. In this case, the observation of MoS$_2$ film underneath the Mo oxide clusters observed in Fig. 2(b) should actually come from the flattened few-layer MoS$_2$ film in front of the Mo oxide clusters. The results of few-layer MoS$_2$ covering the whole sample surface including the Mo oxide clusters suggest that the Mo oxide clusters should form before the formation of the few-layer MoS$_2$ file.

The growth mechanism of MoS$_2$ by using sulfurization of pre-deposited Mo films.
With the results discussed above, a possible growth model for the MoS$_2$ samples prepared by using sulfurization of pre-deposited Mo films is proposed. The schematic diagrams showing the growth evolution of the samples prepared under sulfur sufficient and deficient conditions are shown in Fig. 3(a). After the thin 1 nm Mo deposition, the sample is moved out of the sputtering chamber and exposed to air. The Mo film will be oxidized and form Mo oxides. During the high-temperature growth procedure, the Mo oxide segregation and the sulfurization reaction will take place simultaneously. If the background sulfur is sufficient, the sulfurization reaction will be the dominant mechanism. Most of the surface Mo oxides will be transformed into MoS$_2$ in a short time. The MoS$_2$ film formed on the sample surface will prevent the presence of Mo oxide segregation and coalescence. In this case, a planar MoS$_2$ film will be obtained on the sapphire substrate after the sulfurization procedure. Under the sulfur deficient condition, since there is no sufficient sulfur, only limited numbers of MoS$_2$ will form on the surface. In this case, Mo oxide segregation and coalescence will be the dominant mechanism at the initial stage of the sulfurization procedure. Small Mo oxide clusters are then formed on the sapphire substrates. The thick Mo oxide clusters will prevent complete transformation of the Mo oxides into MoS$_2$. In this case, Mo oxides covered with few-layer MoS$_2$ films will be obtained after the sulfurization procedure. The supporting evidence for the proposed growth model comes from the XPS curves of the two samples measured before and after the sulfurization procedure. The XPS curve of the sample measured before sulfurization is shown in Fig. 3(b). As shown in the figure, Mo^{6+} 3d peaks located at ~235.9 and 232.8 eV and Mo^{4+} 3d peak located at ~229.7 eV are observed. The results indicate that Mo oxides are formed before the sulfurization procedure[23]. The XPS curves measured after the sulfurization procedure for the two samples grown under sulfur sufficient (1.5 g sulfur, blue curve) and deficient (no sulfur supply, red curve) conditions are shown in Fig. 3(c). For the sample grown under the sulfur sufficient condition, the peaks representing Mo^{4+} 3d and S^{2-} 2p orbitals are observed. Due to the spin-orbit interaction, the Mo^{4+}
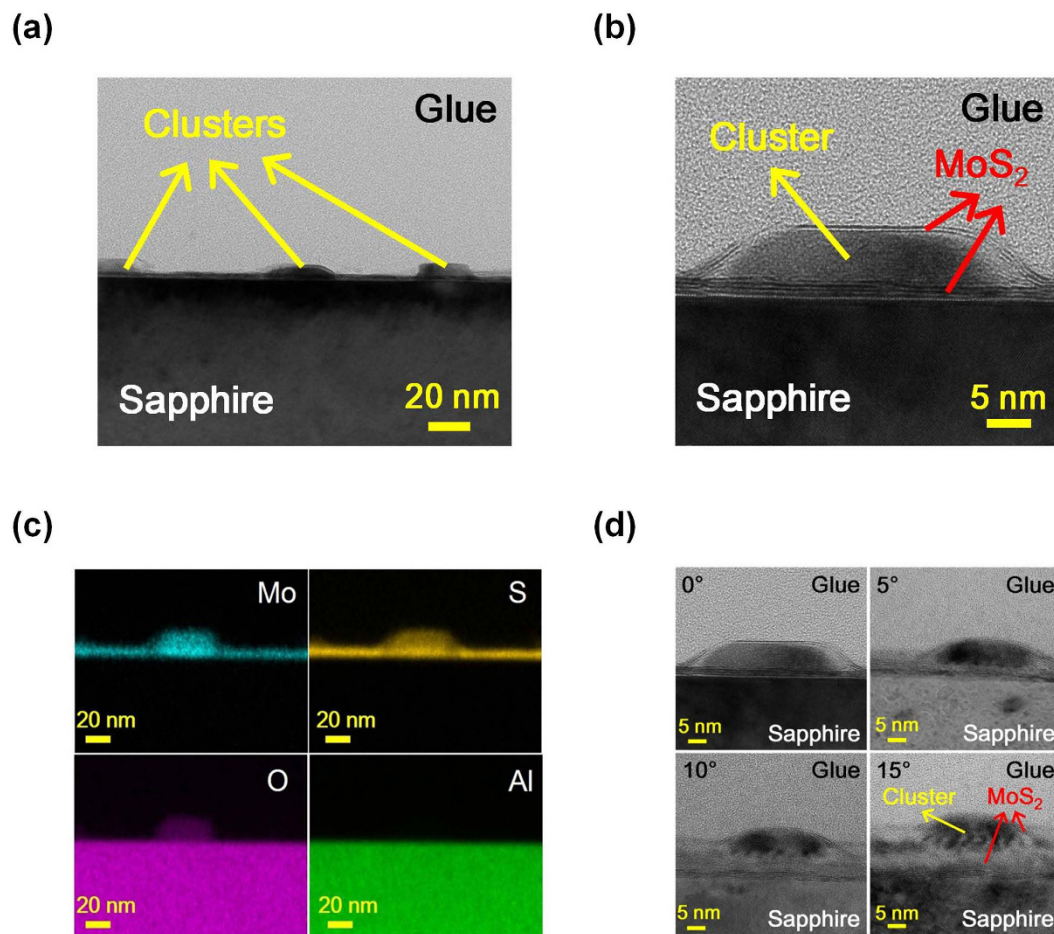
Figure 2. The cross-sectional HRTEM images of the sample prepared with no sulfur supply under (**a**) lower and (**b**) higher magnifications. (**c**) HAADF mappings of elements Mo, S, O and Al and (**d**) the HRTEM images of the same sample with 0°, 5°, 10° and 15° tilt angles from the cross-sectional view.

3d orbital splits into Mo^{4+} $3d_{5/2}$ and Mo^{4+} $3d_{3/2}$ orbitals with binding energies 229.8 and 233 eV, respectively. Similarly, the S^{2-} 2p orbital splits into S^{2-} $2p_{3/2}$ and S^{2-} $2p_{1/2}$ orbitals with binding energies 162.5 and 163.5 eV, respectively[24]. The results suggest that all the Mo oxides have been transformed into MoS_2. However, for the sample prepared under the sulfur deficient condition, beside the Mo^{4+} 3d and S^{2-} 2p peaks, an additional Mo^{6+} 3d peak is also observed. The phenomenon indicates the co-existence of both MoS_2 and Mo oxides after the sulfurization procedure for the sample grown under the sulfur deficient condition. The results have confirmed that depending on the amount of background sulfur, either the Mo oxide segregation or the planar MoS_2 growth will become the dominant mechanism during the sulfurization procedure.

Layer number dependence of MoS_2 on pre-deposited Mo thicknesses and MoS_2 transistors. Layer number controllability is one important issue for the growth of 2D crystals. In previous discussions, it has been predicted that the layer numbers of MoS_2 should be determined by the Mo film thicknesses under the sulfur sufficient condition. To verify this point, two additional samples with 0.2, and 0.5 nm Mo films were prepared and sulfurized under the same sulfur sufficient condition (1.5 g sulfur powder). The cross-sectional HRTEM images of the three samples with pre-deposited 0.2, 0.5 and 1.0 nm Mo films are shown in Fig. 4(a). As shown in the figure, 1-, 3- and 5- layer MoS_2 films proportional to the Mo film thicknesses are obtained for the three samples. The results have confirmed our previous prediction that the MoS_2 layer number is determined by the pre-deposited Mo film thicknesses. The results have also demonstrated that a precise layer number controllability can be achieved by controlling the pre-deposited Mo film thickness. Besides the layer number controllability of this growth technique, for transistor applications, the other important issue is the control of drain current level of the fabricated devices. If similar current transport capacity can be obtained for each MoS_2 layer prepared by using this method, it is possible to determine the required layer number of MoS_2 transistors by simply adding up the drain current value obtained from a single-layer MoS_2 transistor to meet the required drain current level. To verify this point, bottom-gate MoS_2 transistors are fabricated by transferring the 1-, 3- and 5- layer MoS_2 films to 300 nm SiO_2/Si substrates with pre-deposited Au/Ti electrodes[13]. The I_D-V_{GS} curves of the three devices at $V_{DS} = 10$ V are shown in Fig. 4(b). The drain currents for the three device at $V_{GS} = 50$ V are 7, 27 and 35 μA, respectively. The drain currents in positive dependence on the layer numbers of the MoS_2 transistors have
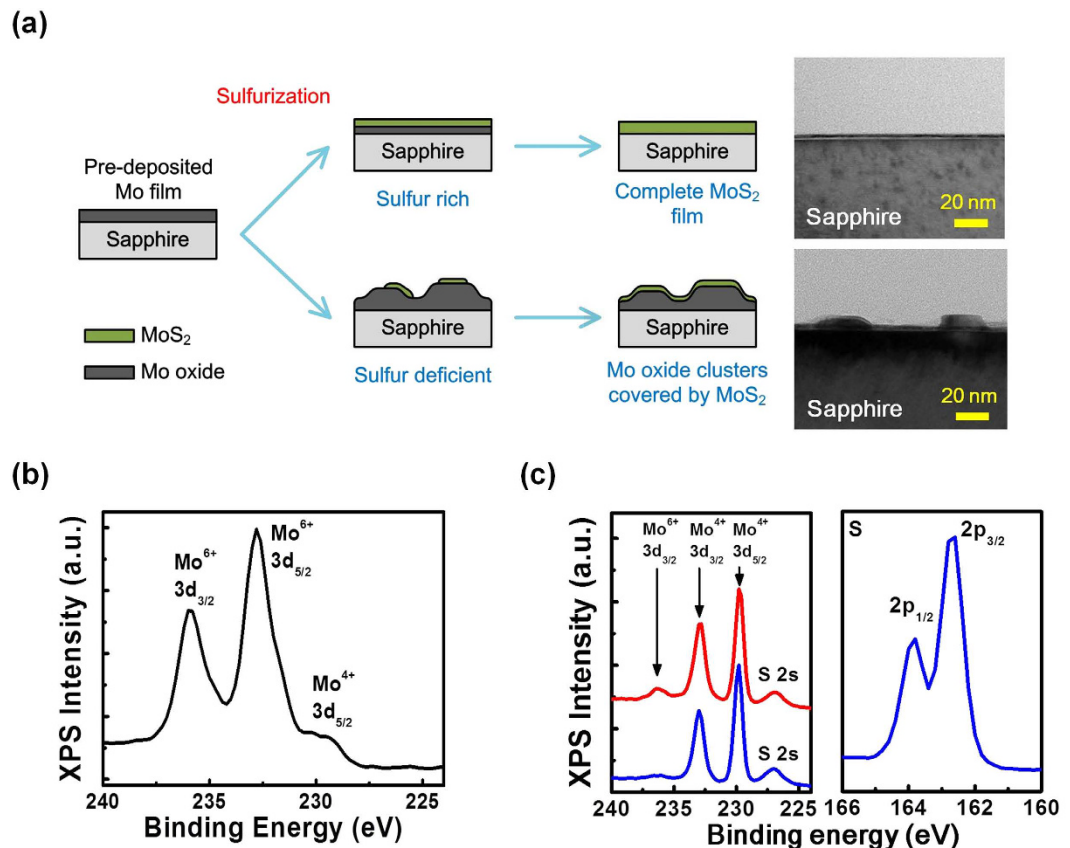
Figure 3. (**a**) The schematic diagrams showing the growth evolution of the samples prepared under sulfur sufficient and deficient conditions. (**b**) The XPS curve measured before the sulfurization procedure. (**c**) The XPS curves measured after the sulfurization procedure for the two samples grown under sulfur sufficient (1.5 g sulfur, blue curve) and deficient (no sulfur supply, red curve) conditions, respectively.
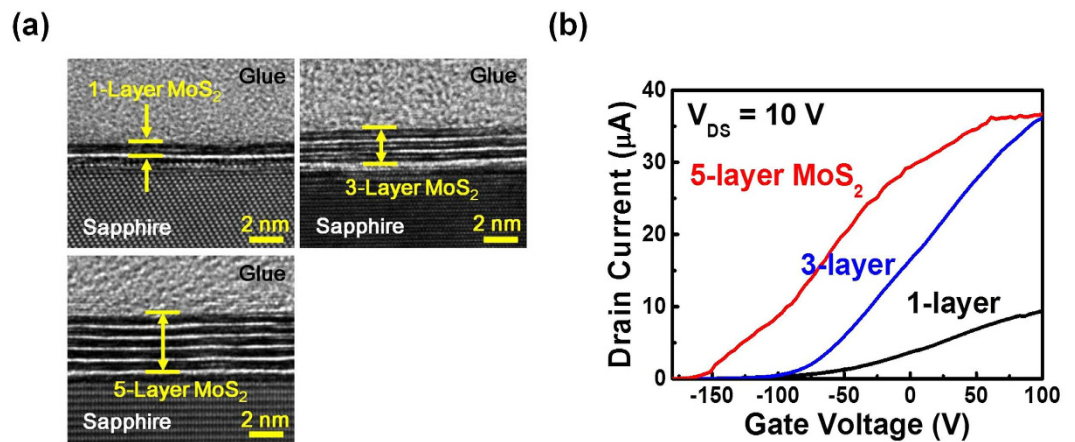
Figure 4. (**a**) The cross-sectional HRTEM images of the three samples with pre-deposited 0.2, 0.5 and 1.0 nm Mo films. 1-, 3- and 5- layers of MoS_2 are obtained for the three samples. (**b**) The I_D-V_{GS} curves of the MoS_2 transistors fabricated by using the three samples measured at $V_{DS} = 10$ V.

demonstrated small variation in material characteristics between each MoS_2 layer prepared by using this growth technique. The results suggest that a better control over the drain current levels may be achieved by controlling the MoS_2 layer numbers after further growth optimization of this growth technique in the future.

The establishment of 2D crystal hetero-structures. The major advantage of TMD growth by sulfurizing pre-deposited transition metals is the possibility of the hetero-structure establishment through similar growth procedures[25,26]. Following the same growth procedure of MoS_2, a WS_2 film is grown after the sulfurization of
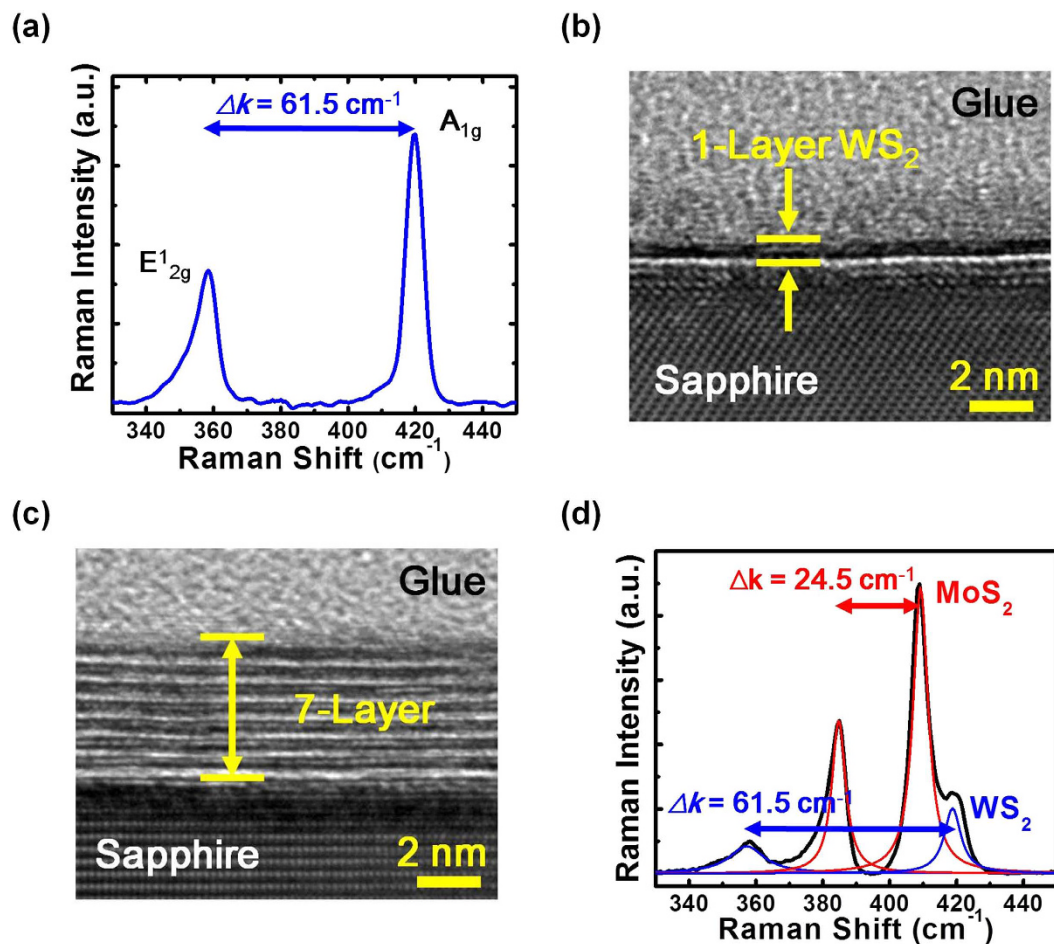
Figure 5. (**a**) The Raman spectrum and (**b**) the cross-sectional HRTEM image of the WS$_2$ sample. (**c**) The cross-sectional HRTEM image and (**d**) the Raman spectrum of the 1-layer WS$_2$/5-layer MoS$_2$/1-layer WS$_2$ double hetero-structure. The fitted characteristic Raman peaks corresponding to the two 2D crystals WS$_2$ and MoS$_2$ are also shown in the figure.

0.5 nm pre-deposited tungsten (W) film on a sapphire substrate. The Raman spectrum of the sample is shown in Fig. 5(a). Similar with MoS$_2$, two characteristic Raman peaks are observed for WS$_2$, which correspond to in-plane E$^1_{2g}$ and out-of-plane A$_{1g}$ phonon vibration modes of the WS$_2$ crystal, respectively. The frequency difference Δk of the two Raman peaks for the WS$_2$ sample is 61.50 cm^{-1}, which is much larger than the Δk value 24.50 cm^{-1} of MoS$_2$. Therefore, it is difficult to predicate the actual layer number of WS$_2$ simply through the Raman spectrum. The cross-sectional HRTEM image of the sample is shown in Fig. 5(b). 1-layer WS$_2$ film is obtained on the sapphire substrate. By sequential depositions of 0.5 nm W, 1.0 nm Mo and 0.5 nm W followed by the same sulfurization procedure after each metal deposition procedure, a WS$_2$/MoS$_2$/WS$_2$ double hetero-structure can be established. Since the layer numbers for WS$_2$ and MoS$_2$ are 1 and 5, respectively, the total layer number for the hetero-structure should be 7. The cross-sectional HRTEM image of the sample with the hetero-structure is shown in Fig. 5(c). As shown in the figure, 7-layer WS$_2$/MoS$_2$/WS$_2$ double hetero-structure is obtained. The results suggest that by sequential metal deposition and the same sulfurization procedures, TMD hetero-structures can be established. The identical layer number of the hetero-structure with the summation of each 2D crystal layer numbers has confirmed the excellent layer number controllability of this growth method. The other supporting evidence for the establishment of the 2D crystal hetero-structure comes from the Raman spectrum of the sample shown in Fig. 5(d). The characteristic Raman peaks corresponding to WS$_2$ and MoS$_2$, respectively, are observed in the figure. Compared with the standalone samples, the same Raman peak differences 24.5 and 61.5 cm^{-1} for MoS$_2$ and WS$_2$ suggest that the same layer numbers are obtained for the two different 2D crystals in the WS$_2$/MoS$_2$/WS$_2$ double hetero-structure.

Conclusion

In summary, we have demonstrated large-area and uniform MoS$_2$ growth by using sulfurization of thin Mo films pre-deposited on sapphire substrates. Precise layer number controllability and the possibility of selective growth of this technique have provided an alternate choice for the growth of large-area and uniform MoS$_2$. We have also proposed a growth model based on the results obtained from the sample grown under the sulfur deficient condition. Depending on the amounts of background sulfur, the competition between the Mo oxide segregation and

the sulfurization reaction is the main mechanism responsible for the growth of either Mo oxide clusters covered with few-layer MoS_2 or planar MoS_2 films after the sulfurization procedure. The positive dependence of drain currents with increasing layer numbers of the 1-, 3- and 5- layer MoS_2 transistors have demonstrated a small variation in material characteristics between each MoS_2 layer prepared by using the sulfurization of pre-deposited Mo films. The demonstration of $WS_2/MoS_2/WS_2$ double hetero-structure has revealed the advantage of this growth technique for the establishment of TMD hetero-structures.

Methods

Before sulfurization, 1 nm of Mo is deposited on sapphire substrates by using a RF sputtering system. During the metal deposition procedure, the sputtering power is kept at 40 W and the background pressure is kept at 5×10^{-3} torr with 40 sccm Ar gas flow. The atomic force microscopy (AFM) image of the sample has revealed that a continuous and smooth film with surface roughness 0.19 nm is obtained after the 1.0 nm Mo deposition. After metal deposition, the samples are placed in the center of a hot furnace for sulfurization. Before sulfurization, the tube is pumped down to 5×10^{-3} torr to evacuate gas molecular such as oxygen from the environment. During the sulfurization procedure, 130 sccm Ar gas was used as carrier gas, while the furnace pressure was kept at 0.7 torr. The growth temperature for the samples was kept at 750 °C with the S powder placed on the upstream of the gas flow. The evaporation temperature for the S powder is kept at 120 °C. Three samples with different amounts of S powder 2.5, 2, and 1.5 g are prepared. An additional sample with no S powder is also prepared for comparison. The Raman spectrums are performed by using a HORIBA Jobin Yvon HR800UV Raman spectroscopy system equipped with 488 nm laser. The cross-sectional HRTEM and HAADF images are obtained by using a FEI Tecnai G2 F20 transmission electron microscopy system operated at 200 kV. The chemical bonds and compositions of the samples are studied by using a PHI VersaProbe II Scanning X-ray photoelectron spectroscopy (XPS) Microprobe.

References

1. Liao, L. *et al.* Sub-100 nm Channel Length Graphene Transistors. *Nano Lett.* **10,** 3952–3956 (2010).
2. Zheng, J. X. *et al.* Sub-10 nm Gate Length Graphene Transistors: Operating at Terahertz Frequencies with Current Saturation. *Sci. Rep.* **3,** 1314 (2013).
3. Wang, Q. H., Kalantar-Zadeh, K., Kis, A., Coleman, J. N. & Strano, M. S. Electronics and optoelectronics of two-dimensional transition metal dichalcogenides. *Nat. Nanotechnol.* **7,** 699–712 (2012).
4. Fiori, G. *et al.* Electronics based on two-dimensional materials. *Nat. Nanotechnol.* **9,** 768–779 (2014).
5. Jariwala, D., Sangwan, V. K., Lauhon, L. J., Marks, T. J. & Hersam, M. C. Emerging Device Applications for Semiconducting Two-Dimensional Transition Metal Dichalcogenides. *ACS Nano* **8** (2014).
6. Cheng, R. *et al.* Few-layer molybdenum disulfide transistors and circuits for high-speed flexible electronics. *Nat. Commun.* **5** (2014).
7. Alam, K. & Lake, R. K. Monolayer MoS_2 Transistors Beyond the Technology Road Map. *IEEE T Electron Dev.* **59,** 3250–3254 (2012).
8. Liu, H., Neal, A. T. & Ye, P. D. D. Channel Length Scaling of MoS_2 MOSFETs. *ACS Nano* **6,** 8563–8569 (2012).
9. Pezeshki, A. *et al.* Top and back gate molybdenum disulfide transistors coupled for logic and photo-inverter operation. *J. Mater. Chem. C* **2,** 8023–8028 (2014).
10. Choi, W. *et al.* High-Detectivity Multilayer MoS_2 Phototransistors with Spectral Response from Ultraviolet to Infrared. *Adv. Mater.* **24,** 5832–5836 (2012).
11. Moldt, T. *et al.* High-Yield Production and Transfer of Graphene Flakes Obtained by Anodic Bonding. *ACS Nano* **5,** 7700–7706 (2011).
12. Lee, Y. H. *et al.* Synthesis of Large-Area MoS_2 Atomic Layers with Chemical Vapor Deposition. *Adv. Mater.* **24,** 2320–2325 (2012).
13. Wu, C. R. *et al.* Multilayer MoS_2 prepared by one-time and repeated chemical vapor depositions: anomalous Raman shifts and transistors with high ON/OFF ratio. *J. Phys. D Appl. Phys.* **48,** 435101 (2015).
14. Lin, M. Y. *et al.* Toward epitaxially grown two-dimensional crystal hetero-structures: Single and double MoS_2/graphene hetero-structures by chemical vapor depositions. *Appl. Phys. Lett.* **105,** 073501 (2014).
15. Choudhary, N. *et al.* Centimeter Scale Patterned Growth of Vertically Stacked Few Layer Only 2D MoS_2/WS_2 van der Waals Heterostructure. *Sci. Rep.* **6,** 25456 (2016).
16. Tao, J. G. *et al.* Growth of wafer-scale MoS_2 monolayer by magnetron sputtering. *Nanoscale* **7,** 2497–2503 (2015).
17. Liu, H. F., Antwi, K. K. A., Ying, J. F., Chua, S. J. & Chi, D. Z. Towards large area and continuous MoS_2 atomic layers via vapor-phase growth: thermal vapor sulfurization. *Nanotechnology* **25,** 405702 (2014).
18. Choudhary, N., Park, J., Hwang, J. Y. & Choi W. Growth of Large-Scale and Thickness-Modulated MoS_2 Nanosheets. *ACS Appl. Mater. Interfaces* 6, 21215–21222 (2014).
19. Orofeo, C. M., Suzuki, S., Sekine, Y. & Hibino, H. Scalable synthesis of layer-controlled WS_2 and MoS_2 sheets by sulfurization of thin metal films. *Appl. Phys. Lett.* **105,** 083112 (2014).
20. Jung, Y. *et al.* Metal Seed Layer Thickness-Induced Transition From Vertical to Horizontal Growth of MoS_2 and WS_2. *Nano Lett.* **14,** 6842–6849 (2014).
21. Li, H. *et al.* From Bulk to Monolayer MoS_2: Evolution of Raman Scattering. *Adv. Funct. Mater.* **22,** 1385–1390 (2012).
22. Laskar, M. R. *et al.* Large area single crystal (0001) oriented MoS_2. *Appl. Phys. Lett.* **102,** 252108 (2013).
23. Wang, J., Li, X., Zhang, S. & Lu, R. Facile synthesis of ultrasmall monodisperse "raisin-bun"-type MoO_3/SiO_2 nanocomposites with enhanced catalytic properties. *Nanoscale* **5,** 4823–4828 (2013).
24. Qin, P. *et al.* *In situ* growth of double-layer MoO_3/MoS_2 film from MoS_2 for hole-transport layers in organic solar cell. *J. Mater. Chem. A* **2,** 2742–2756 (2014).
25. Xue, Y. *et al.* Scalable Production of a Few-Layer MoS_2/WS_2 Vertical Heterojunction Array and Its Application for Photodetectors. *ACS Nano* **10,** 573–580 (2016).
26. Woods. J. M. *et al.* One-Step Synthesis of MoS_2/WS_2 Layered Heterostructures and Catalytic Activity of Defective Transition Metal Dichalcogenide Films. *ACS Nano* **10,** 2004−2009 (2016).

Acknowledgements

Author Contributions

S.-Y. Lin is the group leader and proposed the idea. C.-R. Wu and X.-R. Chang did the material growth and material characterizations. C.-R. Wu, C.-H. Wu and S.-Y. Lin clarified the experimental data and came out with the manuscript.

Additional Information